

Refining Process and Identifying Content of Local Iron Sand

Togar Saragi^{1,a*}, Gustiani A Pramesti^{1,b}, M Abdan Syakuur^{1,c},
Norman Syakir^{1,d}, Sahrul Hidayat^{1,e}, Maykel Manawan^{2,f}, and Risdiana^{1,g}

¹Department of Physics, Padjadjaran University, Jl. Raya Bandung-Sumedang km 21 Jatinangor, Sumedang 45363, Indonesia

²Universitas Pertahanan, Kawasan IPSC Sentul, Sukahati, Kec. Citeureup, Bogor, West Java 16810 Indonesia

^{a*}t.saragi@phys.unpad.ac.id, ^bgustianiarumpramesti@gmail.com, ^cabdan16002@mail.unpad.ac.id,
^dn.sjakir@phys.unpad.ac.id, ^esahrul.hidayat@phys.unpad.ac.id, ^fmaykeltem@gmail.com,
^grisdiana@phys.unpad.ac.id

Keywords: Co-precipitation, iron-sand, magnetite, magnesioferrite, magnesium oxide, ϵ -Fe₂O₃

Abstract. We reported simple processing of local iron sand in order to increase the purity of magnetic phase. The refining process of iron sand is carried out in two stages, namely the iron sand extract using a permanent magnet and the purification process. The purification process was carried out by co-precipitation method in varying of the dissolving temperatures and volume of HCl. The iron salt solution formed is then precipitated using NH₄OH solution and then sintered at 100 °C and 1000 °C, respectively. All samples are characterized by X-ray fluorescence (XRF) and X-ray diffraction (XRD) to identify the elemental content and the crystal structure. From the XRF measurements, it was found that the Fe content before purification process was 32.68 %, increasing to 33.12 % after purification process with HCL volume of 75 ml and sintered at 100 °C. From XRD measurement, it was found that the crystal structure of iron sand before purification process was dominated by magnesioferrite (33.2 %), and magnetite (20.2 %). After purification process at 1000 °C, the magnesioferrite phase increased to 80.2 % and 50.2 % for HCl volume of 50 ml and 75 ml, respectively, while the magnetite phase increase to become 34.5 % for 100 ml of HCl.

Introduction

Indonesia is an archipelago with a very long coastline with an abundance of iron sand. One of the beaches that has great natural potential for iron sand is the southern coast of Java, namely the coast of Kertajati Village, Cianjur Regency, West Java. Iron sand is a metal mining material that is formed due to the transportation and sedimentation process of sand-sized materials containing iron. This iron sand is often found in the form of beach deposits with varying levels, and it was composed of magnetic and non-magnetic minerals. Magnetic minerals are usually either loose or bonded magnetic. One of the minerals contained in this iron sand is magnetite, which can be utilized in a variety of fields. Iron sand is a material that can have high economic value and can even be used as a medicinal material in the medical field. In several countries in the world, iron sand can be found, one of which is New Zealand which is used as a raw material for making steel. Iron sand is not only used as an additional material for cement and steel, but also in the research and development of nanotechnology materials [1–5]. Nanotechnology is a technology that involves atoms and molecules with a size smaller than 100 nanometers. Changes in the size of a material from the bulk scale to the nanoscale can change the physical and chemical properties of a material [6].

This research focuses on refining process of the local iron sand at coast of Kertajati Village, Cianjur Regency, West Java. The aim of this research is to identify the contents of iron sand before and after refining process in various of dissolving of temperature and volume of acid. Several methods in solution phase have been done to synthesize magnetic nanoparticles including isothermal and hydrothermal [3,7]. In this paper, we reported refining process and identification of local iron sand by co-precipitation method. This method is a simple, reliable, and cheap process [8,9].

Experiments

The refining technique of iron sand is carried out in two stages, namely the iron sand extract stage using a permanent magnet and the purification stage using the co-precipitation synthesis method [10,11]. The extraction stage or mechanical decantation was conducted by using a permanent magnet in order to separate of iron sand and soils. The iron sand was then pulverizing to reduce the size and extract by mechanical decantation to improve the quality of iron sand. All iron sand was characterized by XRF and ZRD measurement to investigate the elemental content and crystal structure of iron sand, respectively. The purification process was carried out by co-precipitation method in varying of the dissolving temperatures and volume of HCl. In order to investigate the characteristics of iron sand, the processing was carried out at room temperature by varying the volume of HCl of 50 ml, 75 ml and 100 ml. Hydrochloric acid solution is one of fast-reacting solvent with ferrous metal contained in the iron sand to form iron (II) chloride. Furthermore, the NH_4OH is added dropwise until it reaches pH of 10, and after 17 hours, the iron salt nanoparticles were obtained gravitationally. The iron salt nanoparticles were then washed by n-hexane for three times in the volume ratio of n-hexane and iron sand is 3:1. The resulting samples were then sintered at 100 °C and 1000 °C, respectively. In this experiment, we divided 7 samples, namely Iron San (Irs) refers to raw iron sand after mechanical decantation, Irs-50S100C refers to iron sand dissolving with 50 ml HCl and sintering 100 °C, Irs-75S100C refers to iron sand dissolving with 75 ml HCl and sintering 100 °C, Irs-100S100C refers to iron sand dissolving with 100 ml HCl and sintering 100 °C, Irs-50S1kC refers to iron sand dissolving with 50 ml HCl and sintering 1000 °C, Irs-75S1kC refers to iron sand dissolving with 75 ml HCl and sintering 1000 °C, and Irs-100S1kC refers to iron sand dissolving with 100 ml HCl and sintering 1000 °C All samples are characterized by XRF and XRD to identify the elemental content and the crystal structure.

Result and Discussion

The XRF measurement of elemental content of raw iron sand after mechanical decantation, and after dissolving process in various of the dissolving temperatures and volume of HCl is shown in Table 1. From Table 1, it can be seen that the elemental contents of raw iron sand after mechanical decantation are dominated by Fe, Si, Al, Mg and Ti with m/m percentages contents are 32.68 %, 30.17 %, 19.59 %, 5.59 % and 4.85 %, respectively. The highest content is Fe. The Kertajati's iron sand has very promising prospects for the development of iron materials.

After dissolving process, we obtained the precipitate of iron salt particles. The iron salt precipitation occurs due to the formation of mixed crystals or by adsorption of ions during the precipitation process. This precipitate is the result of the oxidation process of the ferrous metal material contained in the dissolved of iron salt. The elemental content of Fe after purification process and sintered at temperature of 100 °C were 28.31 %, 33.21 % and 27.54 %, while the elemental content of Fe sintering at temperature of 1000 °C was 29.13 %, 31.40 % and 16.47 % with volume of HCl is 50 ml, 75 ml and 100 ml, respectively. The element content of Fe increases by purification process in hydrochloric acid solvent. The highest value of Fe element of 33.12 % was found in sample of Irs-75-S100C, that is sampel dissolve with 75 ml of HCl and sintering at 100°C. On the other hand, the elemental content of Si decreases significantly after purification process, while the elemental content of Ti decreases relatively small, except in sample of Irs-75-1kC, showing an increase of content to 7.84 %. The elemental contents of Al and Mg decreased significantly after purification process at temperature sintered of 100 °C. However, it increases significantly at temperature sintered of 1000 °C. The Al elemen content in sample of Irs-50S1kC was 36.75 %, sample of Irs-75S1kC was 31.44 % and sample of Irs-100S1kC was 34.53 %, while the Mg element content in sample of Irs-50S1kC was 24.25 %, sample of Irs-75S1kC was 24.94 % and sample of Irs-100S1kC was 32.15 %. These high element contents of Fe and Mg will affect the formation of magnetic phase such as magnetite, hematite, and magnesioferrite, as confirmed by XRD measurements. Magnesioferrite is

formed under reducing conditions which occur naturally in the early stages of the hydrothermal process [7].

Table 1. XRF measurement of precipitation in various of the dissolving temperatures and volume of HCl

Element	Iron sand (Irs)	m/m (%)					
		Irs-50-S100C	Irs-75-S100C	Irs-100-S100C	Irs-50-S1kC	Irs-75-S1kC	Irs-100-S1kC
Fe	32.68	28.31	33.12	27.54	29.13	31.40	16.47
Si	30.17	0.541	1.06	0.33	4.04	2.84	3.11
Al	19.59	4.33	6.29	5.63	36.75	31.44	34.53
Mg	5.59	0.26	0.52	-	24.25	24.94	32.15
Ti	4.85	2.87	3.47	2.77	4.29	7.84	4.45
Ca	3.21	0.29	0.58	0.33	0.85	0.53	1.25
Na	2.36	9.45	6.53	9.70	-	-	-
Cl	0.50	53.42	47.79	53.11	0.21	0.33	6.52
K	0.47	-	-	-	-	-	-
Mn	0.24	0.12	0.15	0.11	0.22	0.15	0.10
V	0.23	0.20	0.24	0.20	0.17	0.31	0.24
Zn	0.03	-	-	0.03	0.07	0.14	0.12
Hf	-	0.06	0.06	0.06	-	-	-
Px	-	0.08	0.10	0.11	-	-	-
Cr	-	-	0.03	-	-	0.05	-
Br	-	-	0.03	-	-	-	-

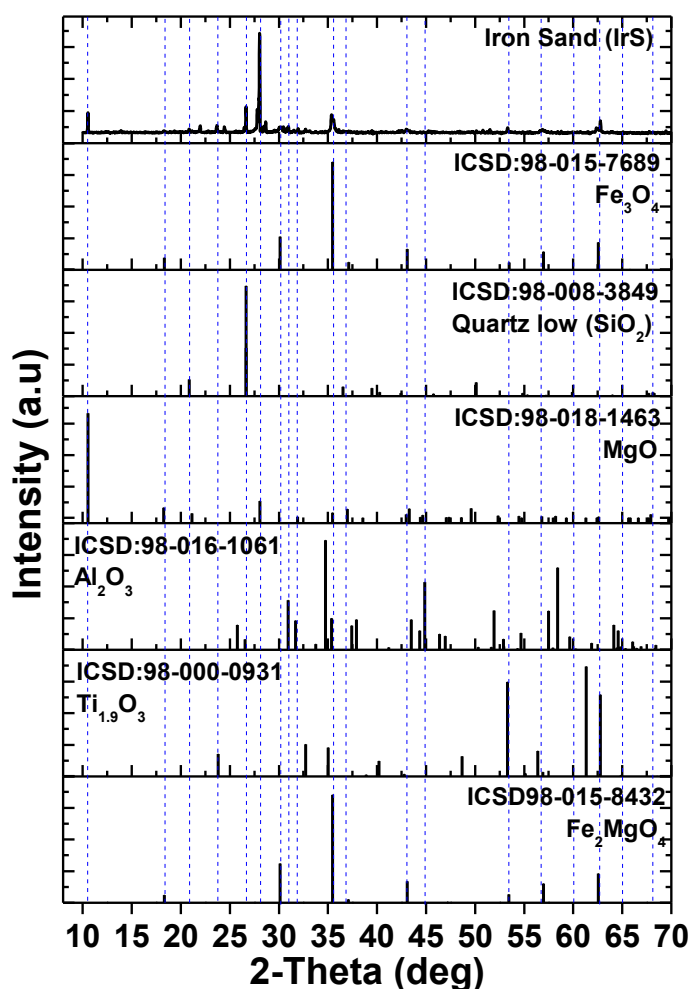


Figure 1. XRD pattern of Iron sand (Irs) after mechanical decantation.

The XRD pattern of raw iron sand after mechanical decantation is shown in Fig. 1. From XRD measurement, it was found that the crystal structure of iron sand (Irs) was dominated by magnesioferrite, magnetite, quartz low and unstable magnesium oxide with match percentage of 33.2 %, 20.2 %, 17.7 % and 15.4 %, respectively as tabulated in Table 2. Table 2 shows the quantitative of match percentage of sample raw iron sand after mechanical decantation.

Table 2. Match percentage of iron sand with the standard data

No	Materials	ICSD	Match (%)
1	Magnetite ($\text{Fe}_{2.929}\text{O}_4$)	98-008-2452	20.2
2	Quartz low (SiO_2)	98-008-3849	17.7
3	Magnesium Oxide-P6/mcc, Unstable (MgO)	98-018-1463	15.4
4	Aluminium Oxide (Al_2O_3)	98-016-1061	7.1
5	Titanium Oxide ($\text{Ti}_{1.904}\text{O}_3$)	98-000-0931	6.3
6	Magnesioferrite (Fe_2MgO_4)	98-015-8432	33.2

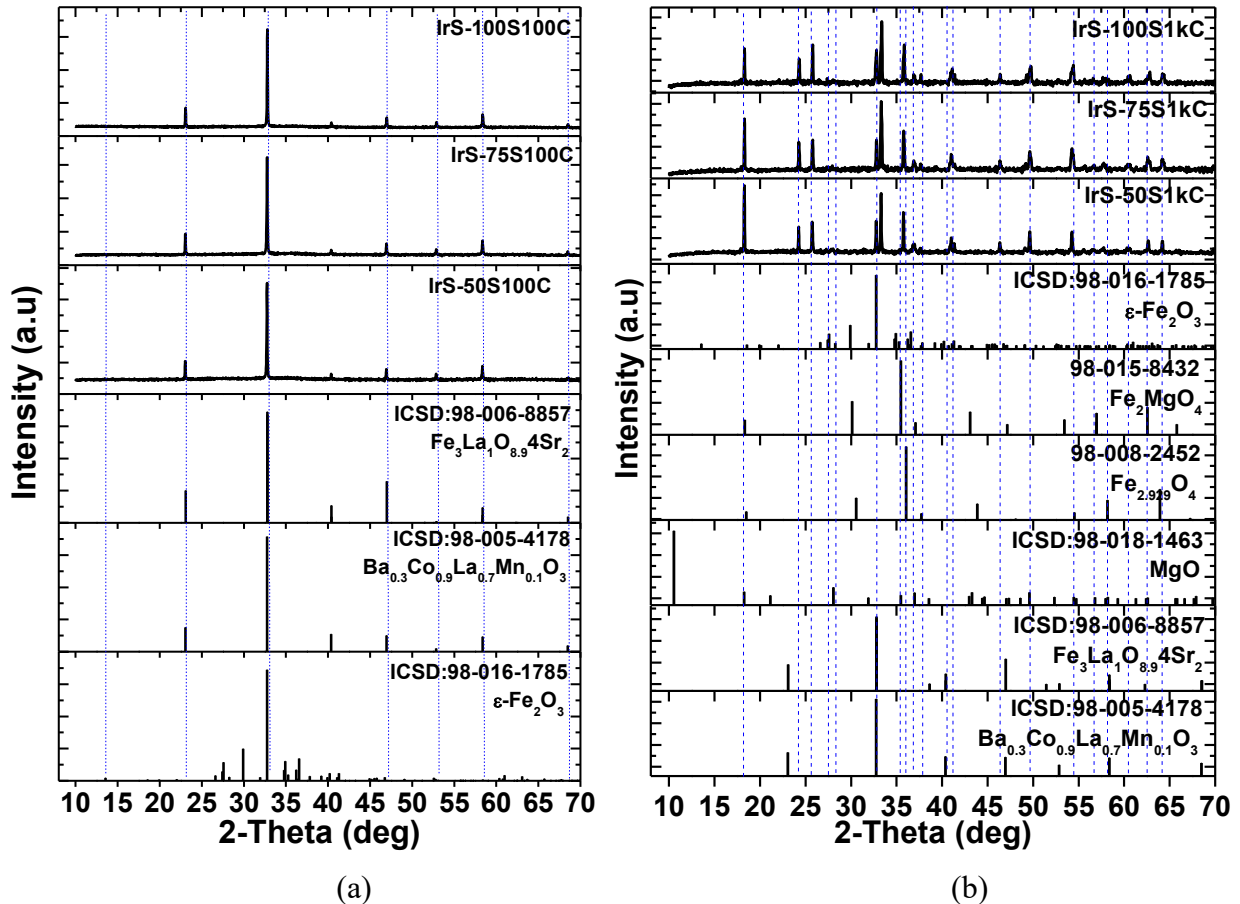


Figure 2. XRD pattern of iron sand with variation volume of HCl of 50 ml, 75 ml and 100 ml sintering at 100 °C (a) and 1000 °C (b).

The XRD pattern of raw iron salt after dissolving with various of HCl volume of 50 ml, 75 ml and 100 ml sintering at 100 °C and 1000 °C is shown in Fig. 2. From Fig. 2(a), it can be seen that the precipitated of iron salt was dominated by Diiron (III) oxide-epsilon nanocrystal ($\epsilon\text{-Fe}_2\text{O}_3$) with the match percentage of 70.5 % for sample of Irs-50-S100C, 51.4 % for Irs-75-S100C, and 49.3 % for Irs-100-S100C, Lanthanum barium cobalt magnesium oxide ($\text{Ba}_{0.3}\text{Co}_{0.9}\text{La}_{0.7}\text{Mn}_{0.1}\text{O}_3$), the match percentage was 20.9 %, 47.3 %, and 49.7 % for samples of Irs-50-S100C, Irs-75-S100C, and Irs-100-

S100C, respectively. The other compound was very small amount less than 1 % for magnesium oxide (MgO), Strontium lanthanum iron oxide ($\text{Fe}_3\text{La}_1\text{Sr}_2\text{O}_{8.94}$), even zero percent for magnetite and magnesioferrite compound, as shown in Table 3. However, generally, magnetite and magnesioferrite highly increased after sintering at 1000 °C as a contribution of elemental contents of Fe and Mg confirmed by XRF measurement shown in Table 1. Table 3 shows the match percentage of iron salt sintered at 100 °C and 1000 °C in various of volume of HCl.

Table 3. Match and semiquantitative percentage of iron sand with the standard data sintering at 100 °C and 1000 °C

No	Materials	ICSD	Match Percentage (%) with various of HCl volume and Ts (°C)					
			HCl:50%		HCl:75 %		HCl:100 %	
			100	1000	100	1000	100	1000
1	Magnesium Oxide-P6/mcc, Unstable (MgO)	98-018-1463	0.6	7.2	1.0	2.6	0.8	35.7
2	Diiron (III) oxide-epsilon nanocrystal ($\epsilon\text{-Fe}_2\text{O}_3$)	98-016-1785	70.5	1.1	51.4	20.2	49.3	20.8
3	Strontium lanthanum iron oxide ($\text{Fe}_3\text{La}_1\text{Sr}_2\text{O}_{8.94}$)	98-006-8857	0	10.6	0.3	0.8	0.1	6.2
4	Lanthanum barium cobalt magnesium oxide ($\text{Ba}_{0.3}\text{Co}_{0.9}\text{La}_{0.7}\text{Mn}_{0.1}\text{O}_3$)	98-0054178	29.0	0.9	47.3	0.4	49.7	1.6
5	Magnetite ($\text{Fe}_{2.929}\text{O}_4$)	98-008-2452	-	0	-	25.8	-	34.5
6	Magnesioferrite (Fe_2MgO_4)	98-015-8432	-	80.2	-	50.2	-	1.2

From Fig. 2(b), it can be seen, that the magnetite and magnesioferrite phase increase by increasing the sintering temperature of 1000 °C. The higher sintering temperature increases the kinetic reaction and maximize the formation of magnetic phase. This increase corresponds to a decrease of the magnesium oxide, strontium lanthanum iron oxide, lanthanum barium cobalt magnesium oxide and diiron (III) oxide-epsilon nanocrystal phase. The match percentage of magnetite phase increased from 0 % for sample of Irs-50-S1kC to 25.8 % for sample of Irs-75-S1kC, and thereafter increased to 34.5 % for sample Irs-100-S1kC. The match percentage of magnesioferrite phase from 80.2 % for Irs-50-S1kC to 50.2 % for Irs-75-S1kC, and down to 1.2 % for Irs-100-S1kC. Decreasing the magnesioferrite and other phase increased the magnetite phase, $\text{Fe}_{2.929}\text{O}_4$. The highest percentage of magnetite (34.5 %) phase was found in sample of Irs-100-S1kC.

Summary

The simple processing of local iron sand has been successfully done in order to increase the purity of magnetic phase. The Fe content before purification process was 32.68 % and increased to 33.12 % after purification process with HCL volume of 75 ml and sintered at 100 °C (Irs-75S100C). The crystal structure of iron sand before purification process was dominated by magnesioferrite (33.2 %), and magnetite (20.2 %), and after purification process the magnesioferrite phase increased to 80.2 % for sampel with HCl volume of 50 ml and sintered at temperature of 1000 °C (Irs-50S1kC) and 50.2 % for sampel with HCl volume of 75 ml and sintered at temperature of 1000 °C (Irs-75-S1kC), while the magnetite phase increased to 34.5 % for samples with 100 ml of HCl and sintered at 1000 °C. The People's Mining Business can use this refining process to improve the economy of the surrounding community.

Acknowledgment

This work was supported by Riset Kompetensi Dosen Unpad (RKDU) 2019 (3rd Year), No. 3331/UN6.D/LT/2019, Pengabdian Kepada Masyarakat Hibah Internal Universitas Padjadjaran Batch I, No. 3450/UN6.D/PM/2019, and partially supported by Academic Leadership Grant of Universitas Padjadjaran 2019, No. 3339/UN6.D/LT/2019. We would like to thanks to Koike Lab, Department of Applied Physics, Graduate School of Engineering Tohoku University Japan for XRD measurements.

References

- [1] E. Park, S. B. Lee, O. Ostrovski, D. J. Min, and C. H. Rhee, Reduction of the Mixture of Titanomagnetite Ironsand and Hematite Iron Ore Fines by Carbon Monoxide, *ISIJ International* 44, 214-216 (2004).
- [2] R. J. Longbottom, B. Ingham, M. H. Reid, A. J. Studer, C. W. Bumby, and B. J. Monaghan, In Situ Neutron Ddiffraction Study of the Reduction of New Zealand Ironsands in Dilute Hydrogen Mixtures, *Mineral Processing and Extractive Metallurgy* 128, 183-192 (2019).
- [3] E. Park, O. Ostrovski, Reduction of Titania-Ferrous Ore by Hydrogen, *ISIJ International* 44, 999-1005 (2004).
- [4] P. L. M. Wong, M. J. Kim, H. S. Kim & C. H. Choi, Sticking Behaviour in Direct Reduction of Iron Ore, *Journal Ironmaking & Steelmaking* 26, 53-57 (1999).
- [5] L. Carter, Ironsand in Continental Shelf Sediments off Western New Zealand—a synopsis, *New Zealand Journal of Geology and Geophysics* 23, 455-468 (1980).
- [6] S. K. Kulkarni, *Nanotechnology: Principles and Practices*, third ed., Springer, New York, 2015
- [7] S. Rajendran, S. Nasir, Hydrothermal altered serpentized zone and a study of Ni-magnesioferrite–magnetite–awaruite occurrences in Wadi Hibi, Northern Oman Mountain: Discrimination through ASTER Mapping, *Ore Geology Review* 62, 211-226 (2014).
- [8] C. Yang, T. Guo, and X. Bian, A new method to prepare water based Fe₃O₄ ferrofluid with high stabilization, *Physica A* 438, 560–567 (2016).
- [9] K. Petcharoen, A. Sirivat, Synthesis and Characterization of Magnetite Co-precipitation Nanoparticles via the Chemical Method, *Materials Science and Engineering B* 177, 421–427 (2012).
- [10] T. Saragi, B. L. Depi, S. Butarbutar, B. Permana and Risdiana, The Impact of Synthesis Temperature on Magnetit Nanoparticles Size Synthesized by Co-Precipitation Method, *Journal of Physics Conf. Series* 1013, 1742 – 6596 (2018).
- [11] T. Saragi, B. Permana, M. Saputri, B. L. Depi, S. W. Butarbutar, L. Safriani, I. Rahayu and Risdiana, The Effect of pH and Sintering Treatment on Magnetic Nanoparticles Ferrite Based Synthesized by Coprecipitation Method, *Journal of Physics Conf. Series* 1080, 012019 (2018).